

Flow Boiling Heat Transfer of R-22 in a Flat Extruded Aluminum Multi-Port Tube

Nae-Hyun Kim[†], Yong-Sup Sim^{*}, Chang-Keun Min^{*}

Department of Mechanical Engineering, University of Incheon, Incheon 402-749, Korea

^{}Graduate School, University of Incheon, Incheon 402-749, Korea*

Key words: Convective boiling, Flat extruded tube, Multi-port tube, Evaporator, R-22

ABSTRACT: Convective boiling heat transfer coefficients of R-22 were obtained in a flat extruded aluminum tube with $D_h=1.41$ mm. The test range covered mass flux from 200 to 600 kg/m²s, heat flux from 5 to 15 kW/m² and saturation temperature from 5°C to 15°C. The heat transfer coefficient curve shows a decreasing trend after a certain quality (critical quality). The critical quality decreases as the heat flux increases, and as the mass flux decreases. The early dryout at a high heat flux results in a unique 'cross-over' of the heat transfer coefficient curves. The heat transfer coefficient increases as the mass flux increases. At a low quality region, however, the effect of mass flux is not prominent. The heat transfer coefficient increases as the saturation temperature increases. The effect of saturation temperature, however, diminishes as the heat flux decreases. Both the Shah and the Kandlikar correlations underpredict the low mass flux and overpredict the high mass flux data.

Nomenclature

<p>A : heat transfer area [mm²] A_c : cross-sectional flow area [mm²] A_i : total internal surface area [mm²] b : thickness of the flat tube [mm] c_p : specific heat [J/kg-K] D_h : hydraulic diameter [mm] D_i : tube inner diameter [mm] g : gravitational acceleration [m/s²] G : mass flux [kg/m²-s] h : heat transfer coefficient [W/m²-K] i_{fg} : latent heat of vaporization [J/kg] k : thermal conductivity [W/m-K] L : length of the test section [mm]</p>	<p>m : mass flow rate [kg/s] Nu_{D_h} : Nusselt number based on hydraulic diameter, $= hD_h/k$ P : pressure [N/m²] Pr : Prandtl number, $= \mu c_p/k$ P_w : wetted perimeter [mm] q : heat flux [W/m²] Q : heat transfer rate [W] Re_{D_h} : Reynolds number based on hydraulic diameter, $= GD_h/\mu_l$ Re_b : Reynolds number for all liquid flow, $= GD_h/\mu_l$ t : tube wall thickness [mm] T : temperature [K] U : overall heat transfer coefficient [W/m²-K] w : width of the flat tube [mm] x : vapor quality</p>
--	---

[†] Corresponding author

Tel.: +82-32-770-8420; fax: +82-32-770-8410

E-mail address: knh0001@incheon.ac.kr

Greek symbols

- μ : dynamic viscosity [kg/m-s]
 ν : kinematic viscosity [m²/s]
 ρ : density [kg/m³]

Subscripts

- ave* : average
meas : measured
i : tube-side
in : inlet
l : liquid
m : mean
o : annular-side
out : outlet
p : pre-heater
pred : predicted
r : refrigerant
sat : saturation
v : vapor
wi : tube-inside

1. Introduction

Fin-and-tube heat exchangers have long been used as evaporators in an air-conditioning system, and rigorous efforts have been made to improve the thermal performance of the heat exchangers. These include a usage of high performance fins, and of small diameter tubes, etc. However, fin-and-tube heat exchangers have inherent short-comings such as contact resistance between fins and tubes, existence of low performance region behind tubes, etc. These short-comings may be overcome if fins and tubes are soldered, and low-profile flat tubes are used. Brazed flat-tube heat exchangers with aluminum louver fins, satisfy the requirements. Such flat-tube heat exchangers have been used as condensers of automotive air-conditioning units for more than ten years, and they are



Fig. 1 Flat extruded aluminum tube ($D_h=1.41$ mm) tested in this study.

seriously considered as evaporators of household air-conditioners.

Cut-away view of a flat tube is shown in Fig.1. Typical widths of flat tubes are 16 to 20 mm, and typical heights are 1 to 3 mm. These tubes have rectangular sub-channels of a small hydraulic diameter (1 to 2 mm). The channel may be smooth or micro-finned. Although several studies were conducted on condensation in flat tubes,⁽¹⁻⁴⁾ only limited studies have been reported on convective boiling in these tubes. Yan and Lin⁽⁵⁾ were the first to run a convective boiling test in a multi-tube geometry. Their multi-tube was made by 28 small diameter tubes ($D_i=2.0$ mm) mounted in a row. The heat was supplied from two copper blocks attached on both sides of the multi-tube. The length of the copper blocks was rather short (10 cm). Using R-134a, they investigated the effects of heat flux ($5 \leq q \leq 15$ kW/m²), mass flux ($50 \leq G \leq 200$ kg/m²s) and saturation temperature ($15^\circ\text{C} \leq T_{sat} \leq 31^\circ\text{C}$). When compared with the data of larger diameter tubes ($D_i \geq 8$ mm), the heat transfer coefficients were 30 to 80% higher. An unexpected 'cross-over' of the convective boiling curve according to the heat flux was observed. At a low quality region, the heat transfer coefficient increased as the heat flux increased. After a certain quality, however, the heat transfer coefficient decreased as the heat flux increased, which resulted in a 'cross-over' of the curves when heat transfer coefficients were plotted against vapor quality with heat flux as a parameter. They explained that, at a high vapor quality, the tube wall may become partly dry when heat flux is high enough. The effect of mass flux was not conclusive.

At a high quality, the heat transfer coefficient increased with the mass flux. At a low quality, however, the heat transfer coefficient for $G=200 \text{ kg/m}^2\text{s}$ was lower than that for $G=100 \text{ kg/m}^2\text{s}$. No acceptable explanation was provided for this unexpected trend. The effect of saturation temperature was also rather complex. At a low heat flux ($q=5 \text{ kW/m}^2$), the heat transfer coefficient decreased as the saturation temperature increased. At a high heat flux ($q=15 \text{ kW/m}^2$), however, the heat transfer coefficient increased as the saturation temperature increased. The reason was attributed to the competing effect of the convection and the bubble generation. At a low heat flux, the convection effect becomes dominant, and yields higher heat transfer coefficient at a lower saturation temperature. At a high heat flux, the bubble generation dominates, which yields higher heat transfer coefficient at a higher saturation temperature. Yan and Lin⁽⁵⁾ also provided the heat transfer and friction correlations based on their data, which were corrected later.⁽⁶⁾

Zhao et al.⁽⁷⁾ reported the CO_2 convective boiling data in a flat tube with $D_h=0.86 \text{ mm}$ having triangular multi-ports. The heat was supplied by providing high electric current through the test section. The effects of heat flux ($3 \leq q \leq 23 \text{ kW/m}^2$), mass flux ($100 \leq G \leq 820 \text{ kg/m}^2\text{s}$) and saturation temperature ($0 \leq T_{sat} \leq 20^\circ\text{C}$) were investigated. The quality-average heat transfer coefficient was almost independent of the mass flux, and increased as the heat flux or the saturation temperature increased. Based on this trend, they concluded that nucleate boiling is the dominant mechanism of heat transfer in CO_2 convective boiling in flat tubes. Later, they⁽⁸⁾ compared the CO_2 convective boiling data with existing correlations, and concluded that none was satisfactory. They developed a correlation, which extended Liu and Winterton⁽⁹⁾ correlation by incorporating a confinement number, proposed by

Cornwell and Kew,⁽¹⁰⁾ to account for the small diameter effect.

Pettersen⁽¹¹⁾ obtained the CO_2 convective boiling data in a flat tube with $D_h=0.81 \text{ mm}$ having circular multi-ports. The heat was supplied by hot water flowing in the annular side of the test section. Data were obtained for the mass flux from 190 to $570 \text{ kg/m}^2\text{s}$, the heat flux 10 to 20 kW/m^2 and the saturation temperature 0°C to 25°C . Heat transfer results showed significant influence of dryout. The critical quality, where dryout occurred, decreased as the heat flux, the mass flux, and the saturation temperature increased. Prior to dryout, the heat transfer coefficients were almost independent of the mass flux, and strongly dependent on the heat flux, which indicates the dominance of nucleate boiling. A heat transfer model was proposed which incorporated the post-dryout model of Shah and Siddiqui.⁽¹²⁾ The onset of dryout was estimated from the water data of Kon'kov.⁽¹³⁾ The model predicted his data with a mean deviation of 35.1%.

Agostini et al.⁽¹⁴⁾ tested two flat tubes of Fig.1 geometry using R-134a. The tubes had different hydraulic diameters, $D_h=0.77 \text{ mm}$ and 2.01 mm . The heat was supplied by providing high electric current through the test section. The heat transfer data showed a significant influence of dryout. The critical quality decreased as the tube diameter decreased. Different from the previous investigators, the heat transfer coefficient was independent of the heat flux (for the test range $4.4 \leq q \leq 14.6 \text{ kW/m}^2$). The heat transfer coefficient was higher for the smaller diameter tube.

Kandlikar and Steinke⁽¹⁵⁾ proposed a heat transfer correlation, which predicts the convective boiling heat transfer coefficient in a mini-channel. The Kandlikar⁽¹⁶⁾ correlation was modified with an appropriate usage of single-phase heat transfer coefficients. They recommended to use laminar heat transfer coefficients when the all-liquid Reynolds number is

less than 1,600. With the modification, some of the Yan and Lin⁽⁵⁾ data were successfully predicted.

The previous survey reveals that convective boiling in a flat tube is very complex. The effects of heat flux, mass flux, etc. are not conclusive yet. The possible flow mal-distribution in multi-port channels may add additional complexity as noted by Webb and Paek.⁽¹⁷⁾ More data are needed to resolve this uncertainty. In this study, convective boiling tests were conducted in a flat tube ($D_h=1.41$ mm) using R-22. The cross-sectional photo of the tube is shown in Fig. 1. The test range covered mass flux from 200 to 600 kg/m²s, heat flux from 5 to 15 kW/m² and saturation temperature from 5°C to 15°C.

2. Experimental apparatus

A schematic drawing of the apparatus is shown in Fig. 2, and a detailed drawing of the test section is shown in Fig. 3. The apparatus and the test section have been used for flat tube condensation tests.⁽⁴⁾ The test section comprises of a flat tube and an annular channel with a length of 455 mm. The refrigerant flows

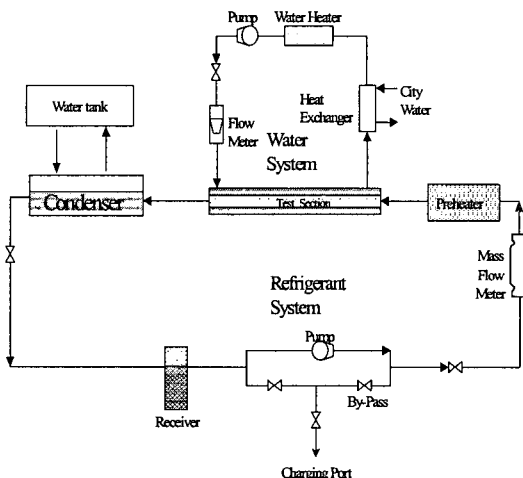


Fig. 2 Schematic drawing of the experimental apparatus.

Table 1 Dimension of the test section

Item	Plain flat tube	
	Tube	Annulus
w (mm)	18.00	20.30
b (mm)	1.70	4.20
A_c (mm ²)	14.72	51.58
$A_i/L(P_w)$ (mm)	41.74	83.97
D_h (mm)	1.41	2.46
t (mm)	0.36	-

inside of the tube and hot water flows in the annular channel. For an accurate measurement of tube-side boiling heat transfer coefficient, it is important to minimize the thermal resistance of the annular side. This may be accomplished by increasing the annular-side water velocity. To increase the water velocity, the annular gap was maintained small (1.0 mm). Geometric details of the tested flat tube and the corresponding annular channel are listed in Table 1.

As illustrated in Fig. 2, the refrigerant flows into the test section at a known quality and partly evaporates in the test section. Two-phase refrigerant mixture from the test section enters the separator, where the liquid drains down to the receiver and the vapor flows into the upper shell-and-tube condenser. The condensed liquid drains down to the receiver. The sub-cooled liquid passes through the magnetic pump, mass flow meter, and enters the pre-heater. The refrigerant flow rate was controlled

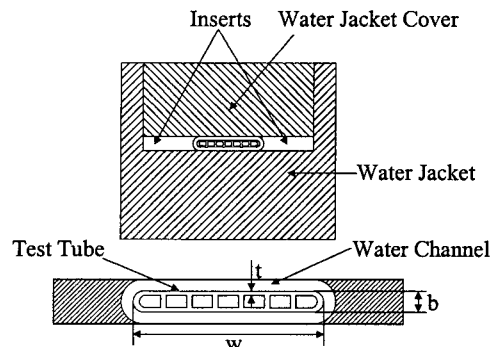


Fig. 3 Detail drawing of the test section.

by by-passing an appropriate amount of liquid. The vapor quality into the test section was controlled by the heat input supplied to the pre-heater. The heat flux to the flat tube was controlled by changing the temperature of heating water. The flow rate of heating water was fixed at 2.0 liter per minute throughout the test.

Temperatures were measured at five locations; refrigerant temperatures at inlet and outlet of the test tube, heating water temperatures at inlet and outlet of the annular channel and a sub-cooled refrigerant temperature at the inlet of the pre-heater. Thermo-wells having five thermocouples each were used to measure local temperatures. Two absolute pressures were measured—one at the inlet of the test section, and the other at the inlet of the pre-heater. These absolute pressures were used to check the state (sub-cooled or saturated) of the refrigerant. A differential pressure transducer was used to measure the pressure drop across the test section. The refrigerant and water flow rates were measured by mass flow meters (Micromotion: DN25S-SS-1) with $\pm 1.5 \times 10^{-6} \text{ m}^3/\text{s}$ accuracy.

The apparatus was checked for leak-tight. Leak tests were conducted by a soap bubble technique followed by a halogen leak detection. The leakage resulted in a decrease in pressure less than 0.5 kPa per hour. The convective boiling test started at the maximum heat flux and mass flux. After the system was stabilized, quality (from 0.1 to 0.9), heat flux (from 5 to 15 kW/m^2) and mass flux (from 200 to 600 $\text{kg}/\text{m}^2\text{s}$), saturation temperature (5°C to 15°C) were sequentially varied, all in a decreasing manner.

3. Data reduction

The tube-side boiling heat transfer coefficient h_i is determined from Eq. (1) using the overall heat transfer coefficient U_o and the annular-side heat transfer coefficient h_o . Here, A_m is the heat transfer area at the middle plane of tube wall.

$$h_i = \frac{1}{\left[\frac{1}{U_o} - \frac{1}{h_o} \right] \frac{A_i}{A_o} - \frac{tA_i}{kA_m}} \quad (1)$$

The annular-side heat transfer coefficient h_o was obtained from the Wilson plot test. To run a Wilson plot test, it is important to maintain both the tube-side and the annular-side turbulent. To promote turbulence at the annular-side, thin wire of 0.3 mm diameter was wrapped around the tube at 3.0 mm pitch. The resulting annular-side forced convection equation is as follows.

$$\text{Nu}_{D_a} = 0.065 \text{Re}_{D_a}^{0.72} \text{Pr}_l^{1/3} \quad (2)$$

To obtain reliable heat transfer data from fluid-to-fluid heat transfer tests such as this one, it is important to minimize the thermal resistance on the Wilson plot-side. For the present test, approximately 30 to 50% of total thermal resistance was on the annular-side. This portion may be reduced by increasing the flow velocity. In that case, however, the temperature difference between inlet and outlet becomes small, and the uncertainty on the calculation of the heat supplied to the test section increases. An approximate optimum annular-side water flow rate was found (2.0 liter per minute) by trial and error resulting corresponding annular-side Reynolds number from 1,000 to 1,700. The smallest water temperature difference from inlet to outlet was 0.65°C , which was observed at the lowest heat flux ($5 \text{ kW}/\text{m}^2$) and mass velocity ($200 \text{ kg}/\text{m}^2\text{s}$).

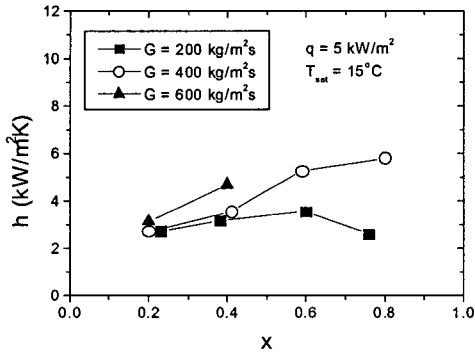
The average vapor quality in the test tube is determined from Eq. (3)

$$x_{ave} = x_{in} + \frac{\Delta x}{2} \quad (3)$$

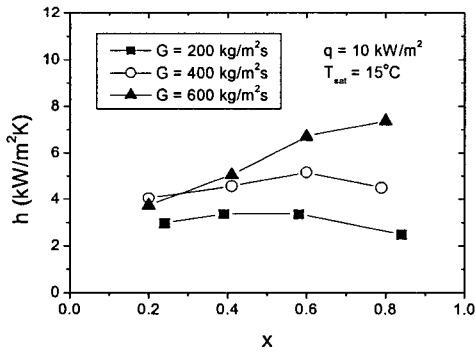
Here, Δx is the change of vapor quality across the test section. The vapor quality into the test section is determined from Eq. (4).

Here, Q_p is the heat supplied to the pre-heater and $T_{p,in}$ is the refrigerant temperature into the pre-heater.

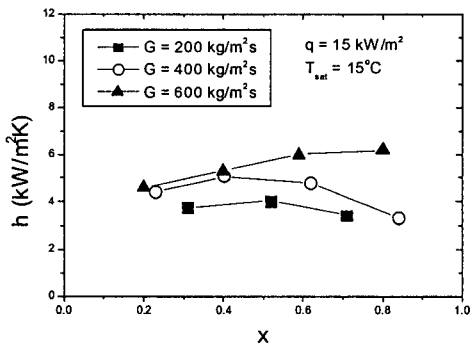
$$x_{in} = \frac{1}{i_{fg}} \left[\frac{Q_p}{m_r} - c_{pr}(T_{sat} - T_{p,in}) \right] \quad (4)$$



(a) $q = 5$ kW/m²



(b) $q = 10$ kW/m²



(c) $q = 15$ kW/m²

Fig. 4 Effect of mass flux on convective boiling heat transfer coefficients.

Experimental uncertainties were analyzed following the method by Kline and McClintock.⁽¹⁸⁾ The uncertainty on the heat transfer coefficient ranged from $\pm 4.7\%$ to $\pm 20.9\%$. The uncertainty increased as the vapor quality increased.

4. Results and discussions

The effect of mass flux on convective boiling of R-22 in the flat tube is shown in Fig. 4. Figure 4(a) is for $q = 5$ kW/m²; Fig. 4(b) for $q = 10$ kW/m² and Fig. 4(c) for $q = 15$ kW/m². The saturation temperature was 15°C . Note that at $G = 600$ kg/m²s and $q = 5$ kW/m², high quality data are not included, because, at that test condition, the thermal resistance ratio on the water-side was too large to accept the data. These graphs show that the heat transfer coefficient increases as the mass flux increases. However, at low quality (below 0.4) of high mass flux ($G = 400$ kg/m²s), the effect of mass flux is negligible. Figure 4 also shows that the slope of the heat transfer coefficient curve decreases gradually as the heat flux increases. The critical qualities, where the heat transfer coefficient curve begins to yield a negative slope, were obtained from the curves, and they are plotted in Fig. 5. The critical quality decreases as the heat flux increases, or as the mass flux decreases. The convective contribu-

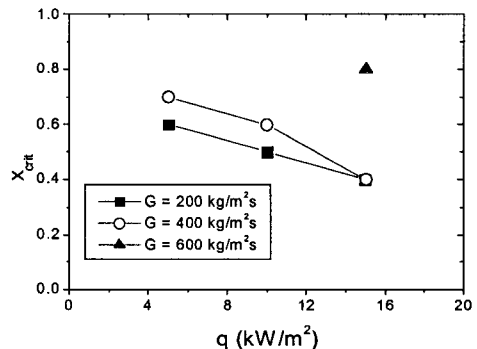


Fig. 5 Effect of mass flux and heat flux on the critical quality.

tion is small at a high heat flux or at a low mass flux, and this may induce an early dry-out. Hapke et al.⁽¹⁹⁾ also observed decrease in the critical quality with the decrease in the mass flux for water and n-heptane boiling in a rectangular channel with 0.3 mm channel width. Pettersen,⁽¹¹⁾ however, observed that the critical quality decreased as the mass flux increased from the CO₂ study. The differences in thermophysical properties (surface tension, density ratio, etc.) between CO₂ and other fluids may be responsible. More investigation on this issue is recommended.

The same data are re-plotted in Fig. 6 to show the effect of heat flux. Figure 6(a) is for $G=200 \text{ kg/m}^2\text{s}$, Fig. 6(b) for $G=400 \text{ kg/m}^2\text{s}$ and Fig. 6(c) for $G=600 \text{ kg/m}^2\text{s}$. At the low mass flux ($G=200 \text{ kg/m}^2\text{s}$) and at a low quality of high mass flux ($G \geq 400 \text{ kg/m}^2\text{s}$), the heat transfer coefficient increases as the heat flux increases. At a high quality of high mass flux, however, the heat transfer coefficient decreases as the heat flux increases. This yields the 'cross-over' of the heat transfer coefficient curves for $G=400 \text{ kg/m}^2\text{s}$ and $G=600 \text{ kg/m}^2\text{s}$. Detailed inspection of the $G=200 \text{ kg/m}^2\text{s}$ curve also shows a 'cross-over' of the $q=5 \text{ kW/m}^2$ and the $q=10 \text{ kW/m}^2$ curves at approximately $x=0.7$. The 'cross-over' of the heat transfer coefficient curve was also reported by Yan and Lin⁽⁵⁾ for R-134a convective boiling in a multi-tube geometry. The 'cross-over' is the result of an early dryout at a high heat flux. The flow mal-distribution at a high heat flux may cause an early dryout as noted by Webb and Paek.⁽¹⁷⁾ The dominance of slug or plug flow in a small diameter channel, as noted by Coleman and Garimella,⁽²⁰⁾ may also be related with the early dryout.

The effect of saturation temperature is shown in Fig. 7 at $G=400 \text{ kg/m}^2\text{s}$. Figure 7(a) is for $q=5 \text{ kW/m}^2$ and Fig. 7(b) for $q=15 \text{ kW/m}^2$. At a low heat flux ($q=5 \text{ kW/m}^2$), the heat transfer

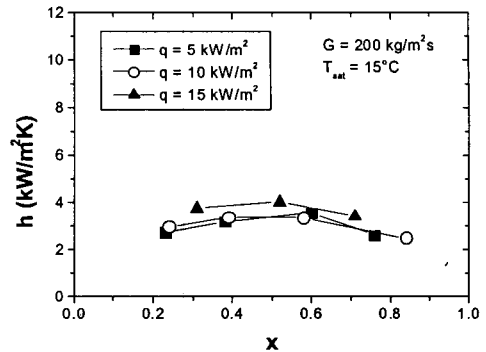
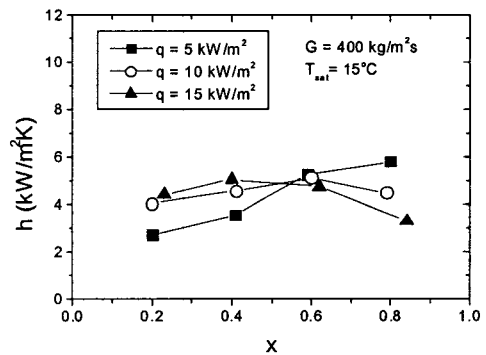
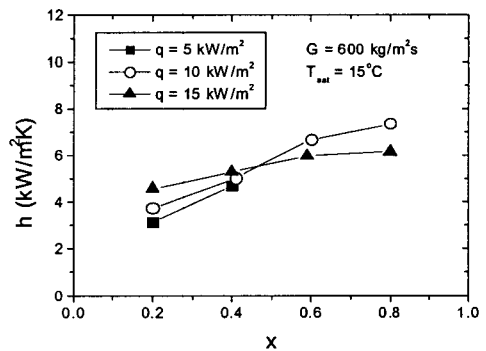
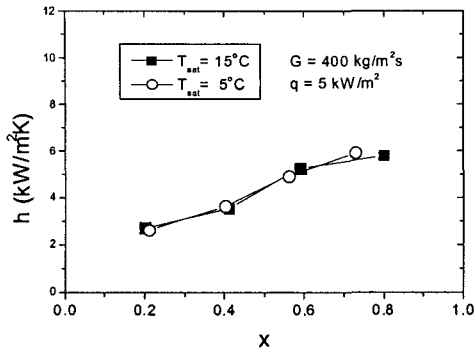
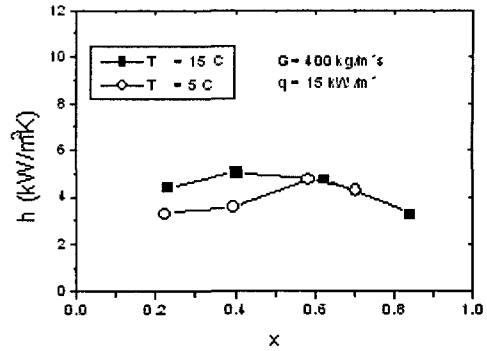
(a) $G=200 \text{ kg/m}^2\text{s}$ (b) $G=400 \text{ kg/m}^2\text{s}$ (c) $G=600 \text{ kg/m}^2\text{s}$

Fig. 6 Effect of heat flux on convective boiling heat transfer coefficients.

coefficient is almost independent of the saturation temperature. At a high heat flux ($q=15 \text{ kW/m}^2$), however, the heat transfer coefficient increases as the saturation temperature increases except for the high quality region. At the high quality region, the heat transfer co-



(a) $q=5\text{ kW/m}^2$



(b) $q=15\text{ kW/m}^2$

Fig. 7 Effect of saturation temperature on convective boiling heat transfer coefficients.

efficients are approximately the same irrespective of the saturation temperature. The reason may be attributed to the dryout, which is obvious from the heat transfer coefficient curves. Figure 7(b) also suggests that the dryout quality decreases as the saturation temperature increases. Similar observation was reported by Pettersen.⁽¹¹⁾ The increase of the heat transfer coefficient with the saturation temperature indicates the nucleate boiling dominance over convection effect. As noted by Zhao et al.,⁽⁷⁾ the Reynolds number in a flat tube is small that the contribution of the convection on the heat transfer is suppressed. At a low heat flux ($q=5\text{ kW/m}^2$), however, the nucleate boiling contribution is also small, and the effect of saturation temperature is negligible.

In Fig. 8, the present data are compared with the Shah⁽²¹⁾ and the Kandlikar⁽¹⁶⁾ correlation. Both correlations require a single-phase heat transfer coefficient to calculate the two-phase convective boiling coefficient. In large diameter tubes, the all-liquid Reynolds number (Re_{lo}) is generally in a turbulent regime, and turbulent heat transfer correlations such as Dittus-Boelter⁽²²⁾ or Petukhov⁽²³⁾ are used to obtain the single phase heat transfer coefficient. In a small diameter tube, however, the Reynolds number could be in a laminar regime, and the application of the turbulent heat transfer correlation may not be appropriate as noted by Kandlikar and Steinke.⁽¹⁵⁾

Kandlikar and Steinke⁽¹⁵⁾ recommend to use a laminar flow correlation when all liquid Reynolds number is less than 1,600. The all liquid Reynolds number of the present study was between 1,700 and 4,800. The literature shows no appropriate single-phase heat transfer correlation in this region.

In the present study, the Gnielinski⁽²⁴⁾ correlation was used to obtain the single phase heat transfer coefficient both for the Shah⁽²¹⁾ and the Kandlikar⁽¹⁶⁾ correlation. Figure 8 shows that both correlations underpredict the low mass flux data (small heat transfer coefficient) and overpredict the high mass flux data (large heat transfer coefficient) with a standard deviation

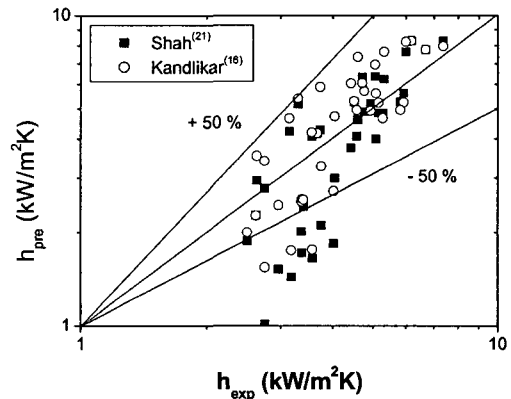


Fig. 8 Comparison of the present data with existing correlations based on large diameter tube data.

–70.8% for the Shah correlation and –70.1% for the Kandlikar correlation.

5. Conclusions

Convective boiling heat transfer coefficients of R-22 were measured in a flat extruded aluminum tube. The test range covered mass flux from 200 to 600 kg/m²s, heat flux from 5 to 15 kW/m², and saturation temperature from 5°C to 15°C. Listed below are major findings.

(1) The heat transfer coefficient curve shows a decreasing trend after a certain quality (critical quality). The critical quality decreases as the heat flux increases, and as the mass flux decreases. The small convective contribution at a high heat flux or at a low mass flux may induce an early dryout in the tube.

(2) The early dryout at a high heat flux results in a unique ‘cross-over’ of the heat transfer coefficient curves.

(3) The heat transfer coefficient increases as the mass flux increases. At a low quality region, however, the effect of mass flux is not prominent.

(4) The heat transfer coefficient increases as the saturation temperature increases. This trend diminishes as the heat flux decreases.

(5) Both the Shah and the Kandlikar correlations underpredict the low mass flux and overpredict the high mass flux data.

References

1. Katsuta, M., 1994, The effect of a cross-sectional geometry on the condensation heat transfer inside multi-pass Tube, Proc. WTPF, POSTECH, Vol. 2, pp. 245-252.
2. Yang, C. Y. and Webb, R. L., 1996, Condensation of R-12 in small hydraulic diameter extruded aluminum tubes with and without micro-fins, Int. J. Heat Mass Trans., Vol. 39, pp. 791-800.
3. Koyama, S., Kuwahara, K., Nakashita, K. and Yamamoto, K., 2002, An experimental study on condensation of R134a in a multi-port extruded tube, Proceedings of 2002 International Refrigeration Conference at Purdue, R6-2.
4. Kim, N.-H., Cho, J.-P., Kim, J.-O. and Youn, B., 2003, Condensation heat transfer of R-22 and R-410A in flat aluminum multi-channel tubes with or without microfins, Int. J. Refrigeration, Vol. 26, pp. 830-839.
5. Yan, Y.-Y. and Lin, T.-F., 1998, Evaporation heat transfer and pressure drop of refrigerant R-134a in a small pipe, Int. J. Heat Mass Transfer, Vol. 41, pp. 4183-4194.
6. Yan, Y.-Y. and Lin, T.-F., 2003, Letter to the editors; Reply to Prof. R.L. Webb and J.W. Paek's Comments, Int. J. Heat Mass Transfer, Vol. 46, pp. 1111-1113.
7. Zhao, Y., Molki, M. and Ohadi, M. M., 2000, Heat transfer and pressure drop of CO₂ flow boiling in microchannels, Proceedings of the ASME Heat Transfer Division, HTD-Vol. 366-2, Vol. 2, pp. 243-249.
8. Zhao, Y., Molki, M. and Ohadi, M. M., 2001, Predicting flow boiling of CO₂ in microchannels, Proceedings of 2001 International Mechanical Engineering Congress and Exposition, HTD-Vol. 369-3, IMECE2001/HTD-24216, pp. 205-210.
9. Liu, Z. and Winterton, R. H. S., 1991, A general correlation for saturated and subcooled flow boiling in tubes and annuli based on a nucleate pool boiling equation, Int. J. Heat Mass Transfer, Vol. 34, pp. 2759-2766.
10. Cornwell, K. and Kew, P. A., 1993, Boiling in small parallel channels, in energy efficiency in process technology, ed., P. A. Pilavachi, New York, Elsevier, pp. 624-638.
11. Pettersen, J., 2003, Two-phase flow pattern, heat transfer and pressure drop in micro-channel vaporization of CO₂, ASHRAE Transactions, Vol. 109, Pt. 1, CH-03-8-1.
12. Shah, M. M. and Siddiqui, M. A., 2000, A general correlation for heat transfer during

- dispersed-flow film boiling in tubes, *Heat Transfer Engineering*, Vol. 21, No. 4, pp. 18-32.
13. Kon'kov, A. S., 1965, Experimental study on the conditions under which heat exchange deteriorates when a steam-water mixture flows in heated tubes, *Teploenergetika*, Vol. 13, No. 2, p. 77.
 14. Agostini, B., Bontemp, A., Watel, B. and Thonon, B., 2003, Boiling heat transfer in mini-channels: influence of the hydraulic diameter, *International Congress of Refrigeration 2003*, Washington D. C., ICR0070.
 15. Kandlikar, S. G. and Steinke, M. E., 2003, Predicting heat transfer during flow Boiling in minichannels and microchannels, *ASHRAE Transactions*, Vol. 109, Pt. 1, CH-03-13-1.
 16. Kandlikar, S. G., 1990, A general correlation for saturated two-phase flow boiling heat transfer inside horizontal and vertical tubes, *J. Heat Transfer*, Vol. 112, pp. 219-228.
 17. Webb, R. L. and Paek, J. W., 2003, Letter to the editors; Discussions on Y.-Y. Yan and T.-F. Lin's paper, *Int. J. Heat Mass Transfer*, Vol. 46, pp. 1111-1113.
 18. Kline, S. J. and McClintock, F. A., 1953, The description of uncertainties in single sample experiments, *mechanical engineering*, Vol. 75, pp. 3-9.
 19. Hapke, I., Boye, H. and Schmidt, J., 2000, Flow boiling of water and n-heptane in micro-channels, in heat transfer and transport phenomena in microscales, G.P. Celata et al., eds., Begell House, Inc., pp. 222-228.
 20. Coleman, J. W. and Garimella, S., 1999, Characterization of two-phase flow patterns in small diameter round and rectangular tubes, *Int. J. Heat Mass Trans.*, Vol. 42, pp. 2869-2881.
 21. Shah, M. M., 1976, A new correlation for heat transfer during boiling flow through pipes, *ASHRAE Trans.*, Vol. 82, Pt. 2, pp. 66-86.
 22. Dittus, F. W. and Boelter, L. M. K., 1930, Heat transfer in automobile radiators of a tubular type, university of california publication on engineering, Vol. 2, p. 433.
 23. Petukhov, B. S., 1970, Heat transfer in turbulent pipe flow with variable physical properties, in *advances in heat transfer*, eds. T. F. Irvine and J. P. Hartnett, Academic Press, Vol. 6, pp. 504-564.
 24. Gnielinski, V., 1976, New equations for heat and mass transfer in turbulent pipe and channel flow, *International Chemical Engineering*, Vol. 16, pp. 359-368.